




Electrochemically synthesized green fluorescent carbon dots for quantitation of hypochlorite and carbendazim

Follow this and additional works at: <https://www.jfda-online.com/journal>

 Part of the [Food Science Commons](#), [Medicinal Chemistry and Pharmaceutics Commons](#), [Pharmacology Commons](#), and the [Toxicology Commons](#)



This work is licensed under a [Creative Commons Attribution-NonCommercial-No Derivative Works 4.0 License](#).

Recommended Citation

Lo, Kuan-Min; Lin, Yu-Shen; Liou, Je-Wen; Chiu, Tai-Chia; and Hu, Cho-Chun (2023) "Electrochemically synthesized green fluorescent carbon dots for quantitation of hypochlorite and carbendazim," *Journal of Food and Drug Analysis*: Vol. 31 : Iss. 2 , Article 4.

Available at: <https://doi.org/10.38212/2224-6614.3445>

This Original Article is brought to you for free and open access by Journal of Food and Drug Analysis. It has been accepted for inclusion in Journal of Food and Drug Analysis by an authorized editor of Journal of Food and Drug Analysis.

Electrochemically synthesized green fluorescent carbon dots for quantitation of hypochlorite and carbendazim

Kuan-Min Lo ^a, Yu-Shen Lin ^a, Je-Wen Liou ^b, Tai-Chia Chiu ^a, Cho-Chun Hu ^{a,*}

^a Department of Applied Science, National Taitung University, Taitung, Taiwan

^b Department of Biochemistry, School of Medicine, Tzu Chi University, Hualien, Taiwan

Abstract

Green emission carbon dots (CDs) electrochemically prepared from 2,6-pyridinedicarboxylic acid and o-phenylenediamine were applied separately for the quantitation of hypochlorite and carbendazim. The characteristic and optical properties of the CDs were studied through fluorescence, UV-vis absorption, X-ray photoelectron spectroscopy, and transmission electron microscopy. The synthesized CDs were mainly 0.8–2.2 nm in size, with an average size of 1.5 nm. The CDs exhibited green luminescence centered at 520 nm when excited by 420 nm light. The green emission of the CDs is quenched after the addition of hypochlorite, mainly through the redox reaction between hypochlorite and hydroxyl groups on the CDs surface. Furthermore, the hypochlorite-induced fluorescence quenched can be prevented in the presence of carbendazim. The sensing approaches exhibit good linear ranges of 1–50 μM and 0.05–5 μM for hypochlorite and carbendazim, respectively, with low detection limits of 0.096 and 0.005 μM , respectively. Practicalities of the luminescent probes were separately validated by the quantitation of the two analytes in real sample matrix with recoveries ranging from 96.3 to 108.9% and the relative standard deviation values below 5.51%. Our results show the potential of the sensitive, selective, and simple CD probe for water and food quality control.

Keywords: Carbendazim, Carbon dots, Electrochemical synthesis, Hypochlorite

1. Introduction

Carbon dots (CDs), one of the popular nanomaterials, have recently been widely applied in sensing of metal ions, drugs, amino acids, and pesticides [1–10] because of their unique fluorescent and chemical affinity properties. Now many bottom-up approaches to synthesis of CDs have been developed, including thermal routes, microwave-assisted methods, hydrothermal and aqueous-based methods, electrochemical, and ultrasonic-assisted synthesis, [11,12]. Among these methods, electrochemical synthesis offers simple, low-cost, low-pressure operations that can be performed at room temperature [1]. Furthermore, it allows simple control of the size and functional group of the CDs to conveniently modify and customize their optical and chemical properties, making it with great development potential.

Disinfection is an important part water treatment process in cities [13]. Hypochlorite is an important reactive oxygen species with strong oxidation capability, which has been used in household bleaching [14] and water disinfection [15]. However, excessive exposure of human skin to hypochlorite can cause a series of symptoms like allergies [16]. Additionally, the excessive accumulation of HOCl/CIO⁻ may result in all kinds of inflammation-related diseases, such as neuron degeneration [17], atherosclerosis [18], osteoarthritis [19], and renal disease [20]. Therefore, it is of great practical significance to develop a rapid and sensitive method to detect hypochlorite in water.

Carbendazim (CBZ) is a kind of benzimidazole fungicide. It is extensively used to prevent and control numerous diseases in crops, fruits, and vegetables [21]. Recently, CBZ abuse has been reported in Taiwan,

Received 6 September 2022; accepted 18 October 2022.
Available online 15 June 2023

* Corresponding author.

E-mail addresses: alan112601@gmail.com (K.-M. Lo), cangeroo@nttu.edu.tw (Y.-S. Lin), jwliou@mail.tcu.edu.tw (J.-W. Liou), tcchiu@nttu.edu.tw (T.-C. Chiu), cchu@nttu.edu.tw (C.-C. Hu).

<https://doi.org/10.38212/2224-6614.3445>

2224-6614/© 2023 Taiwan Food and Drug Administration. This is an open access article under the CC-BY-NC-ND license (<http://creativecommons.org/licenses/by-nc-nd/4.0/>).

mainly because of its low price and wide range of effectiveness. When applied to soils, CBZ can remain for a long time because its benzimidazole ring is difficult to be broken down, and consequently, its degradation is slow [22,23]. As a result, the risk of CBZ residues in crops, water, and soil, poses a threat to agricultural production and human health [24]. Additionally, it has been reported that CBZ can disrupt spermatogenesis and decrease reproduction in mammals [25]. Moreover, CBZ exposure can impair liver function, leading to hepatic lipid metabolism disorder, and alter the enzyme activity in mammals [26]. The methods most frequently used for measuring benzimidazole fungicides are high-performance liquid chromatography [27], mass spectroscopy [28], UV–vis absorption [29], fluorescence spectroscopy [30] and electrochemical techniques [31]. Although these methods have brilliant responses to CBZ, the design of new nanomaterials is still needed to accelerate the development of a highly sensitive pesticide sensing platform.

In this study, CDs were synthesized electrochemically from 2,6-pyridinedicarboxylic acid (DPA) and o-phenylenediamine (oPD) as shown in Scheme 1. The prepared CDs were separately used to detect hypochlorite and CBZ. Hypochlorite induces fluorescence

quenching of the CDs, which can be restored in the presence of CBZ as also shown in Scheme 1. Our results revealed that the prepared CDs exhibited excellent photoluminescence properties, good biocompatibility, low toxicity, and low cost.

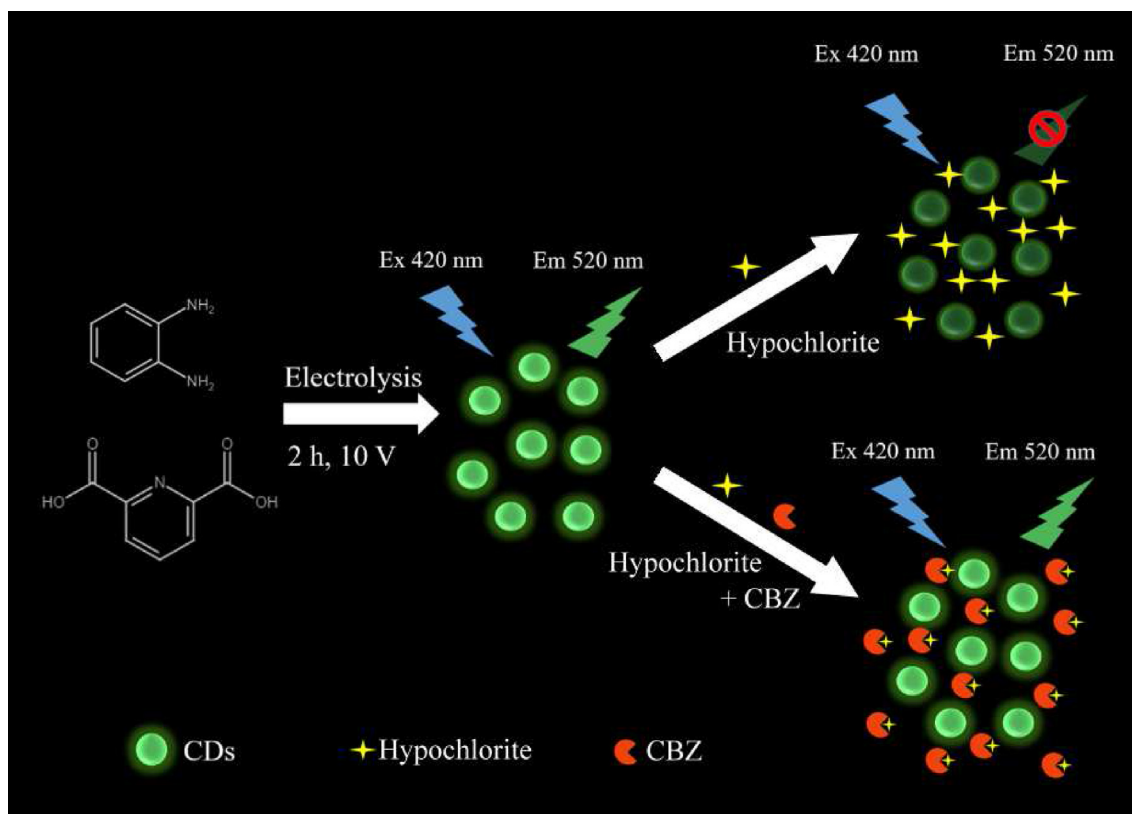
2. Materials and methods

2.1. Materials

Carbon precursors including DPA and oPD were obtained from Alfa Aesar (USA). Other chemicals were purchased from Sigma–Aldrich. (USA) All reagents were analytical grade and used directly without any further purification. Ultrapure water with a resistivity of $\geq 18.25 \text{ M}\Omega/\text{cm}$ was used throughout the experiment. The probe purification was carried out using 3500 Da cutoff membranes (Amicon Ultra-4, Millipore).

2.2. Apparatus

The electrolysis for CDs preparation was conducted using a bespoke apparatus (Kaishin Co., Ltd, Taiwan). Fluorescence measurements were performed by using a Shimadzu RF-6000 spectrofluorophotometer.



Scheme 1. Schematic diagrams showing (a) the preparation of CDs, (b) fluorescent detection of hypochlorite and CBZ.

The ultraviolet–visible (UV–vis) spectra were obtained by a Hitachi U-2900 UV–vis spectrophotometer (Tokyo, Japan). The transmission electron microscope (TEM) images were taken on a PHILIPS CM-200 TWIN TEM (Amsterdam, Netherlands). X-ray photoelectron spectroscopy (XPS) was measured by a Thermo K-Alpha (Thermo Fisher, USA.). Zeta potential measurements were performed on a Zetasizer Nano-ZS90 (Malvern, UK).

2.3. Synthesis of the green fluoresces CDs

The CDs were synthesized by an easy and one-step electrochemical method. DPA (0.16712 g) and oPD (0.1622 g) were added to 0.2 M NaOH solution (15 mL) to form a transparent solution under stirring. Two platinum wires (6 cm × 0.1 cm) were employed as the positive and negative electrodes with a distance of about 1 cm. The reaction proceeded for 2 h at a potential of 10 V (DC). After 2 h, the solution turned from transparent to dark brown. The solution was centrifuged at 10000 g at 15 °C for 10 min to remove large particles. The obtained dark brown solution was filtered through a microporous filtering film (0.22 μm). The colloidal solution was repeatedly dialyzed against ultrapure water in a dialysis bag (3500 Da) for 6 h. The dark brown solution was obtained and stored at 4 °C.

2.4. Detection of hypochlorite and carbendazim using the CDs

The detection of hypochlorite was performed at room temperature in pH 7.0, 10 mM phosphate buffer solution (PBS). Different concentrations of hypochlorite (200 μL each) were separately added into the mixture of 80 μL of the CDs solution, 1520 μL of ultrapure water, and 200 μL of PBS (pH 7.0). The above mixture was shaken for 30 min. The fluorescence spectra were recorded under excitation at the wavelength of 420 nm. In order to detect the specificity of the CDs to the hypochlorite, the tested anions were used instead of hypochlorite under the same condition. All the experiments were performed at room temperature.

The detection of CBZ was performed at room temperature in pH 7.0, 10 mM PBS. First, aliquots of 50 μM of hypochlorite (200 μL each) were separately added into different concentrations of CBZ solution before 200 μL of PBS (pH 7.0) and ultrapure water was added to make each mixture with a final volume of 1920 μL. After vigorously shaking for 30 min, 80 μL of the CD was added (final 2 mL) and shaken for 5 min. The fluorescence spectra were recorded under excitation at 420 nm. To detect the specificity

of the CD to the CBZ, the other pesticides were used to replace CBZ and the analysis was conducted under the same condition. All the experiments were performed at room temperature.

2.5. Analysis of real samples

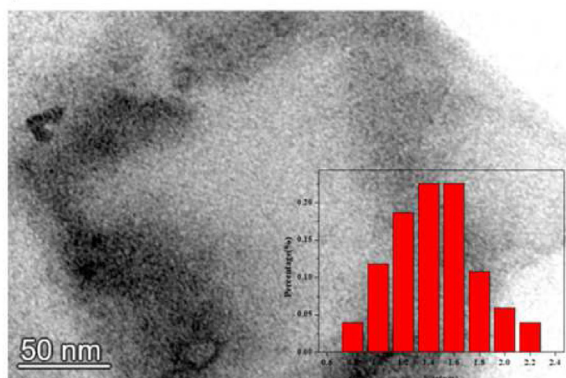
Drinking water and mineral water samples were employed to demonstrate the practicality of the CD sensor for hypochlorite detection. The mineral water sample was collected from convenience stores located in the campus of National Taitung University (NTTU), and drinking water was collected from the water dispenser on the NTTU campus. The collected water samples were spiked separately with hypochlorite standard solution, filtered through a 0.22 μm membrane, and diluted with ultrapure water (10-fold dilution). Then, the fluorescence spectra were measured on the spectrophotometer after incubating with CDs probe for 30 min. White rice samples were purchased from a local store. LC-MS/MS was applied to the analysis of the rice samples, showing non-existence of any pesticides. The white rice samples were all prepared according to the QuEChERS method [32]. The rice samples were grinded into small pieces. The homogenized sample (5 g) was separately added to 10 mL of ultrapure water containing various amounts of CBZ (5, 20, and 40 μM). After being equilibrated for 10 min, 10 mL of acetonitrile solution containing 1% acetic acid, 4 g MgSO₄, and 1 g CH₃COONa was added. After being shaken vigorously for 1 min, the mixture was subjected to centrifuge at 3000 g for 1 min. Each of the supernatant (6 mL) was added to a centrifuge tube containing 0.3 g primary secondary amine (PSA), 0.3 g C18, and 0.9 g MgSO₄. After being shaken vigorously for 1 min, the mixture was centrifuged at 3000 g for 2 min. Each of the supernatant (2 mL) was dried under a nitrogen stream and then re-dissolved in 2 mL of ultrapure water. Finally, the prepared white rice sample was diluted 100 times with ultrapure water and quantified using the aforementioned method.

3. Results and discussion

3.1. Synthesis and characterization of CDs

The CD was synthesized through electrochemical processing for 2 h with a DC voltage of 10 V. According to the literature, we suggested that the formation of CDs at the anode is initiated from the oxidation of oPD to form radicals that further react with DPA and oPD through condensation, polymerization, carbonization, and passivation [4,6,33].

(A)



(B)

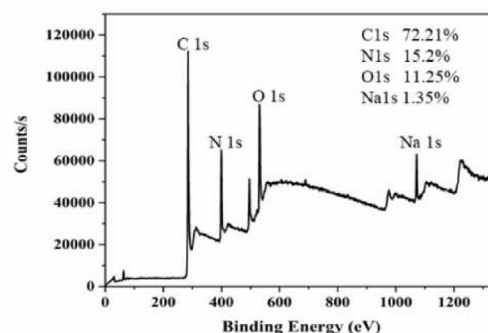


Fig. 1. (A) TEM image of CDs and (B) XPS survey spectrum. [Inset to (A): the size distribution for CDs].

To obtain CDs with the most appropriate fluorescence properties, we investigated the molar ratio ranging from 0:1.5 to 2:1.5 of the two carbon precursors, DPA and oPD. From the results listed in Table S1 (<https://www.jfda-online.com/journal/vol31/iss2/4/>), the CD synthesized at the DPA and oPD ratio of 1:1.5 exhibited the strongest green fluorescent intensity at 520 nm when excited at 420 nm, and thus it was selected to develop sensitive and selective probes in this study. TEM image (Fig. 1A) shows that the CDs are spheroidal with an average diameter of approximately 1.5 nm (25 counts), with a narrow size distribution as shown in the inset. The chemical structure of the CD was

investigated through X-ray photoelectron spectroscopy (XPS) as shown in Fig. 1B. Three peaks at 284.6, 399.6, and 531.6 eV correspond to C1s, N1s, and O1s. The CD consists of C (72.21%), N (15.2%), and O (11.25%). Fig. S1A (<https://www.jfda-online.com/journal/vol31/iss2/4/>) shows the C1s spectrum. The three peaks at 284.8, 286.0, and 288.4 eV reveal the presence of C–C/C=C [34], C–N [35], and –COO [35], respectively. In the high-resolution of N1s spectrum, two peaks at 399.25 and 400.5 eV are assigned for amino N and pyrrolic N [36,37] (Fig. S1B) (<https://www.jfda-online.com/journal/vol31/iss2/4/>). As shown in Fig. S1C (<https://www.jfda-online.com/journal/vol31/iss2/4/>), three peaks

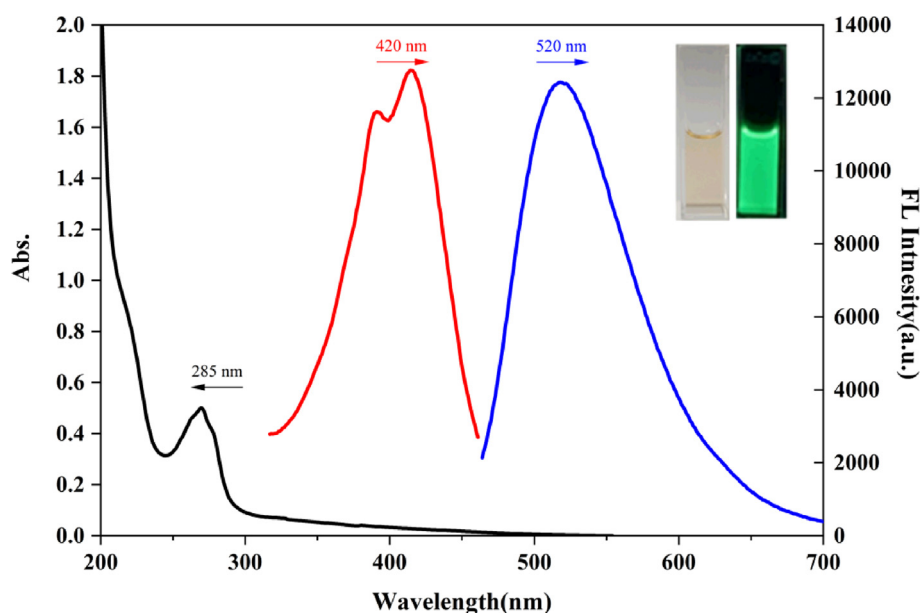


Fig. 2. UV–Vis absorption (black), excitation (red) and emission (blue) spectra of CDs. [Inset: photographs of CDs in visible-light (left) and under UV-light ex 365 nm (right)].

Table 1. Determination of ClO^- concentrations in spiked water samples using CDs ($n = 5$).

Sample	Spiked (μM)	Found (μM)	Recovery (%)	RSD (%)
Drink water	5	5.06	101.2	5.47
	20	20.91	104.5	4.38
	40	43.59	108.9	4.07
Mineral water	5	4.97	99.5	3.45
	20	19.27	96.3	5.51
	40	40.59	101.4	4.65

located at 531.2, 532.5, and 535.5 eV confirm the existence of $\text{C}=\text{O}$ [38], $\text{C}-\text{OH}$ [39], and $-\text{COOH}$ [40] respectively.

3.2. Optical properties of the CDs

The optical characteristics of these CDs were investigated through UV/vis absorption and fluorescence spectroscopy. The absorption peak at 285 nm (Fig. 2) is due to the $\pi-\pi^*$ transition of aromatic sp^2 domains from the carbon core. The

emission spectrum shows the greatest green emission located at 520 nm and the excitation spectrum displays the maximum excitation wavelength occurring at 420 nm. Additionally, the CD dispersion under irradiation with a portable UV-light (emission wavelength of 365 nm) exhibits a strong green emission.

The effect of ionic strength on the fluorescence intensity was investigated by treating CD with various concentrations of sodium chloride (0.1–1 M) at pH 7.0. Fig. S2A (<https://www.jfda-online.com/>

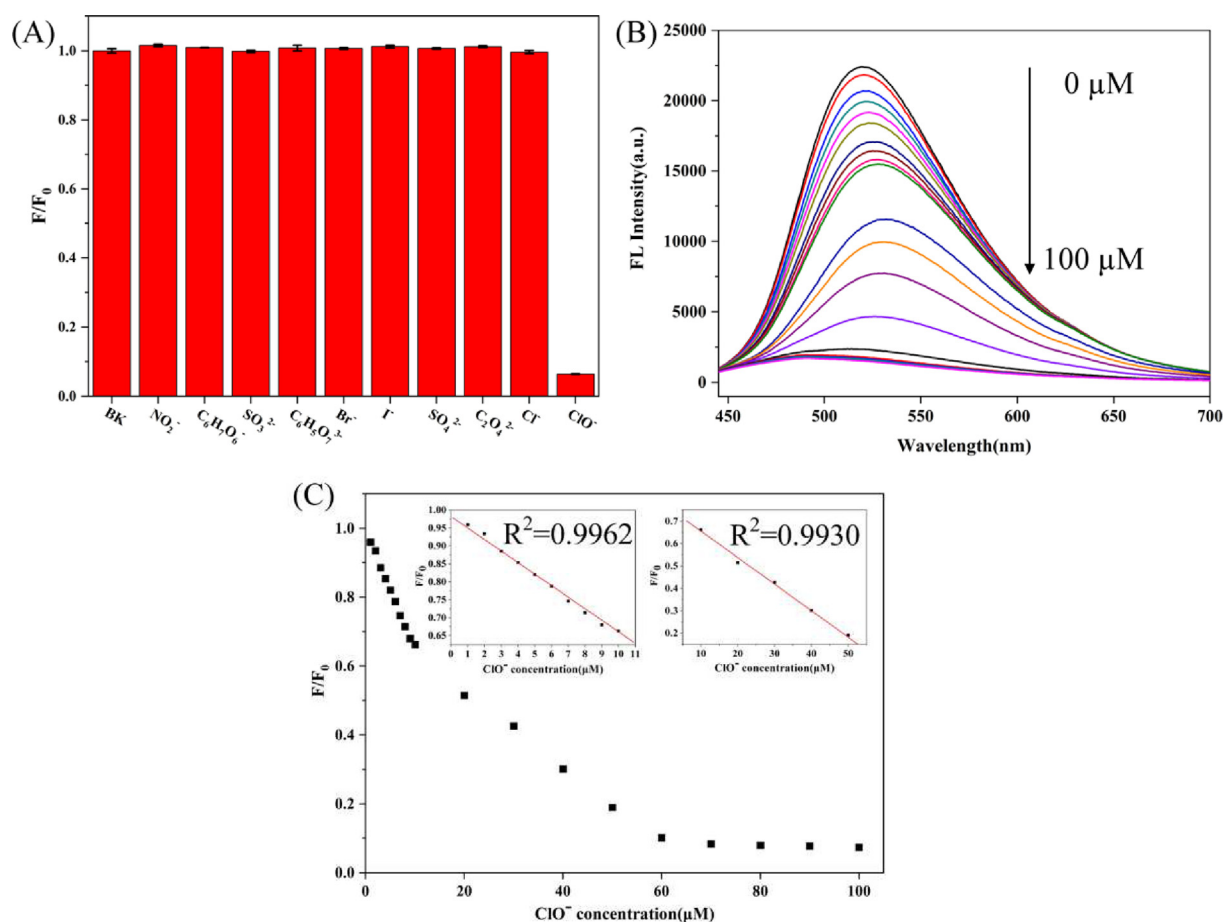


Fig. 3. Fluorescence response of CDs after addition of (A) different oxidizing/reducing agents, (B) different concentrations of ClO^- , and (C) relative fluorescence intensities (F/F_0) of CDs treated with various concentrations of hypochlorite. [Insets to (C): Two calibration curves of CDs for sensing ClO^-].

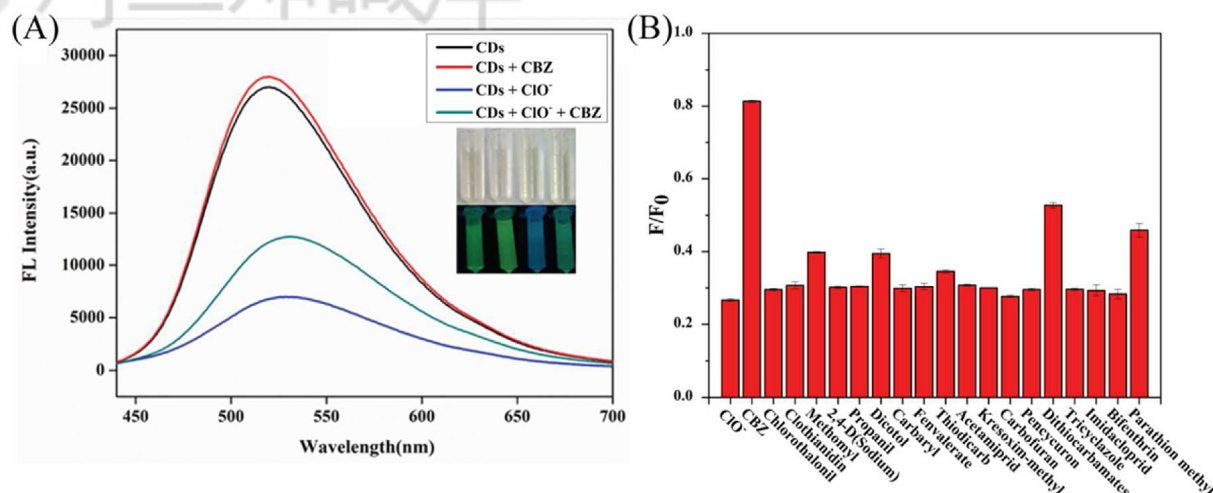


Fig. 4. (A) Fluorescence spectra of CDs, CDs/CBZ, CDs/CIO⁻, and CDs/CIO⁻ + CBZ. (B) Selectivity of the CDs/CIO⁻ probes toward CBZ over the tested pesticides. Inset: Photographs of CDs, CDs/CBZ, CDs/CIO⁻, and CDs/CIO⁻ + CBZ in visible-light (up) and under UV-light emitted at 365 nm (down). The concentrations of CBZ and CIO⁻ are 50 μ M (10 ppm) and 50 μ M, respectively. The concentrations for all the tested pesticides are 10 ppm.

journal/vol31/iss2/4/) displays that the emission intensity is almost the same (<6%) even at high sodium chloride concentrations (>1.0 M), showing their great potential for biological and environmental applications. Next, we investigated the resistance of our CDs to photobleaching through UV-light illumination. As shown in Fig. S2B (<https://www.jfda-online.com/journal/vol31/iss2/4/>), under continuous UV-light (365 nm) illumination for 1 h, the CD's emission fluorescence intensity at 520 nm only changes slightly (<25% variation). Furthermore, as shown in Fig. S2C (<https://www.jfda-online.com/journal/vol31/iss2/4/>), the intensity of green emission remained stable in solutions at various pH values (6.0–12.0). Having such stable physical and optical properties, the obtained CDs are good candidates to

be further developed as probes for the analysis of biological samples.

3.3. Quantitation of hypochlorite

Fig. 3A and Fig. S3 (<https://www.jfda-online.com/journal/vol31/iss2/4/>) show the effect of tested oxidizing/reducing agents (all 100 μ M) on the fluorescence intensity at 520 nm of the CD colloidal solution (10 mM PBS, pH 7.0). Among these tested chemical reagents, only hypochlorite caused the fluorescence quenching of CDs. We believed that this quenching was caused by the reaction between hypochlorite and the functional groups such as aromatic amines possessed on the surface of the CD [41–43]. As shown in Fig. 3B, the fluorescence

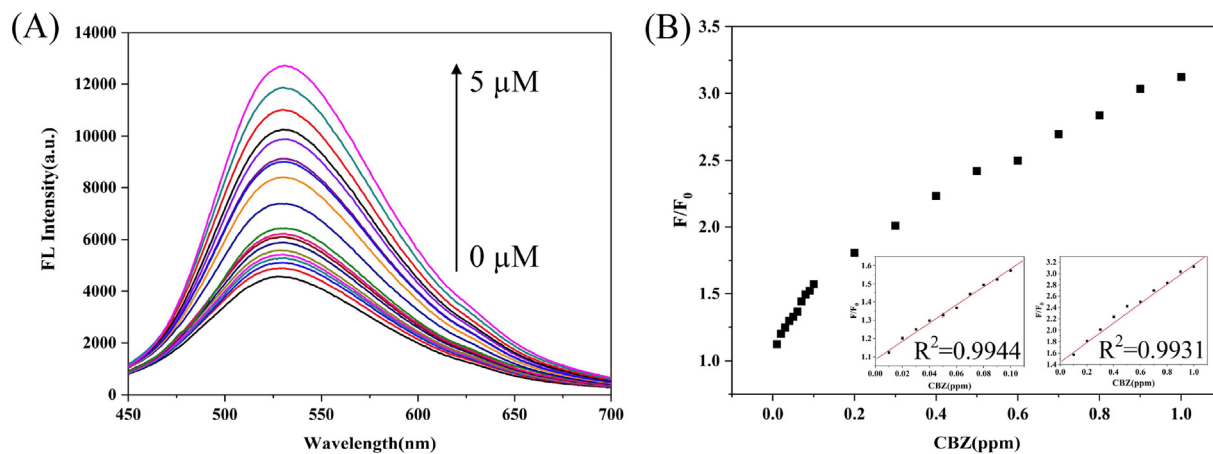


Fig. 5. (A) The fluorescence response of CDs/CIO⁻ system versus different concentrations of CBZ, (B) the fluorescent response of CDs/CIO⁻ system versus different concentrations of CBZ. [Inset: The calibration curve of CDs/CIO⁻ system for sensing CBZ].

Table 2. Determination of CBZ in rice sample using CD/CIO⁻ probe and compared with LC-MS/MS. (n = 5).

Probe	CD/CIO ⁻				LC-MS/MS	
	Spike(ppm)	Found(ppm)	Recovery(%)	RSD(%)	Found(ppm)	Recovery(%)
rice	0.025	0.0264	105.6	1.4	0.0252	100.8
	0.05	0.0538	107.7	2.0	0.0497	99.4
	0.1	0.103	103.1	3.2	0.1014	101.4

intensity of the CD probes gradually decreased with increasing the hypochlorite concentration ranging from 0 to 100 μM . Meanwhile, two excellent linear relationships ($R^2 = 0.993$ and 0.9962) were performed between the fluorescent intensity ratio (F/F_0) and the hypochlorite concentration, ranging from 1 to 10 μM and 10 to 50 μM , respectively. The regression equations are $F/F_0 = -0.3216 [\text{ClO}^-] + 0.98232$ and $F/F_0 = -0.01185 [\text{ClO}^-] + 0.77443$. Based on the $3\sigma/S$ (where σ represents the standard deviation of the blank, and S represents the slope of the calibration curve), LOD

was calculated to be $0.096 \mu\text{M}$, which is lower than most probes (Table S2) (<https://www.jfda-online.com/journal/vol31/iss2/4/>) [44–47]. Two linear regions are believed due to the oxidation of surface functional groups and core chemical bonds [43]. Having the advantages of stability, sensitivity, and selectivity, we further applied the CD probe for sensing of hypochlorite in real water samples. As shown in Table 1, satisfactory recoveries were obtained at 96.3–108.9% for the spiked water samples at various concentrations (5, 20, and 40 μM). The value of the RSD below 5.51% demonstrated the reliability and accuracy of

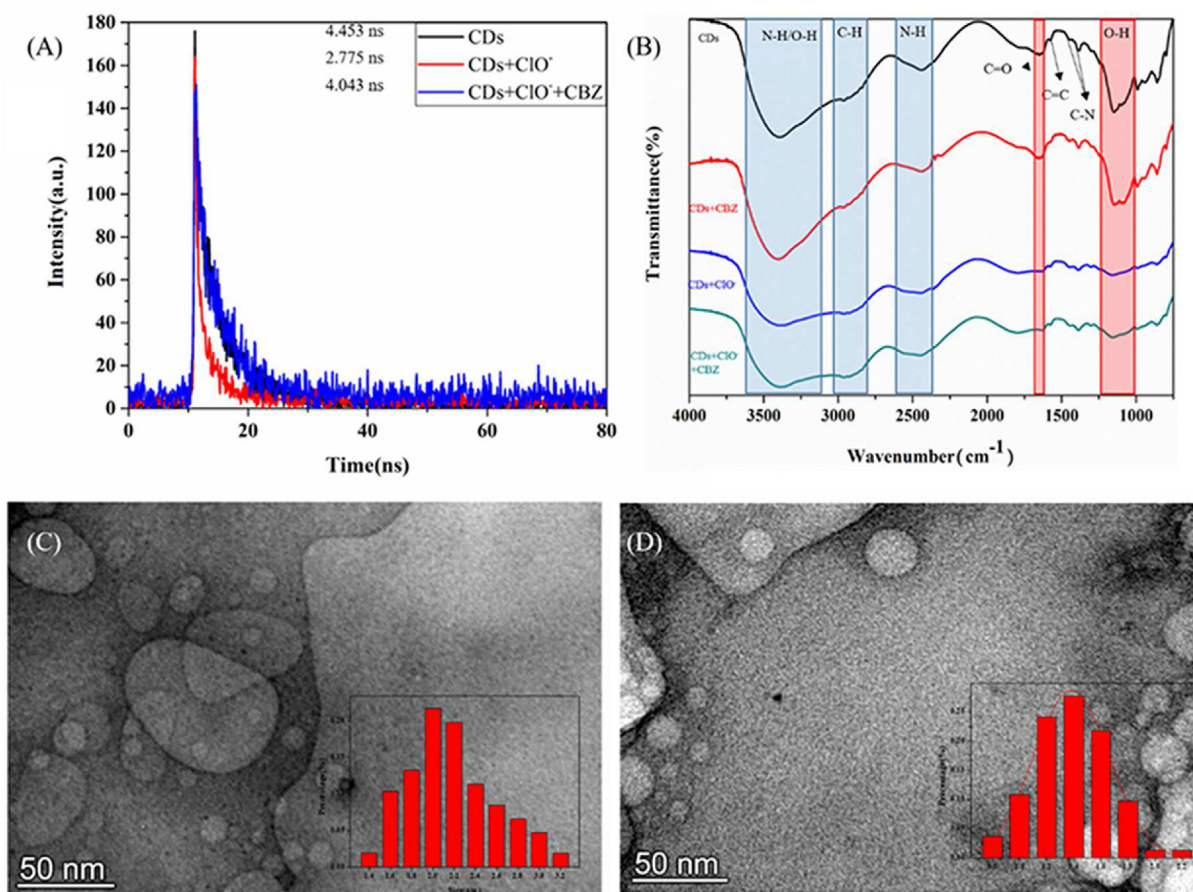


Fig. 6. (A) Fluorescence intensity decay curves of CDs (black), CDs + ClO⁻ (red), and CDs/ClO⁻ + CBZ, (B) FT-IR spectra of CDs (black), CDs + CBZ (red), CDs + ClO⁻ (blue), and CDs/ClO⁻ + CBZ (green), (C) TEM image of CDs/ClO⁻ (D) TEM images of CDs/ClO⁻ + CBZ. Insets to (C) and (D): Size distribution of CDs/ClO⁻ mixtures in the absence (C) and presence of CBZ (D).

this CD fluorescence sensor. Therefore, a green and convenient method has been developed to detect hypochlorite in environmental samples.

3.4. Quantitation of carbendazim

As shown in Fig. 4A, addition of CBZ and hypochlorite mixtures (50 μM) to CD solution, considerable fluorescence from the CD was observed. Among the tested pesticides, only CBZ and dithiocarbamate suppressed fluorescence quenching induced by hypochlorite as shown in Fig. 4B, mainly because they reacted with hypochlorite. The fluorescence intensity of the CD at a constant concentration of hypochlorite increased upon the addition of CBZ in various concentrations (0–5 μM) as shown in Fig. 5A. There are also two linear relationships in the concentration ranges of 0.05–0.5 μM (0.01–0.1 ppm), and 0.5–5 μM (0.1–1 ppm). The linear equations are $F/F_0 = 4.87 [\text{CBZ}] + 1.09$ and $F/F_0 = 1.63 [\text{CBZ}] + 1.54$, with R^2 values of 0.9931 and 0.9944, respectively, where F and F_0 represent separately the fluorescence intensities of the CD in the presence and absence of CBZ. The LOD ($3\sigma/S$) is 0.005 μM . Various concentrations of CBZ (0.1, 1, and 2 μM) were added to both the water and rice samples for the real sample application. For the spiked water samples, satisfactory recoveries were achieved at 96.3–108.9% as shown in Table 2. The RSD values all below 5.51% reveal the reliability and accuracy of this CD fluorescence sensor. Furthermore, the data from our sensor are not significantly different from that obtained from the traditional standard method (LC-MS/MS). With its simplicity, this sensor is suitable for rapid screening of CBZ in the farm or market to ensure the safety of agriculture products.

3.5. Quenching and recovery mechanism of CDs

The fluorescence lifetimes decay curves of CDs were collected and shown in Fig. 6A to propose the quenching mechanism of CDs induced by hypochlorite, which is suppressed by CBZ. The lifetimes were found to be 4.45 ns in the absence of both CBZ and hypochlorite, 2.77 ns in the presence of hypochlorite, and 4.04 ns in the presence of CBZ/hypochlorite. These results suggested that the fluorescence quenching of CDs induced by hypochlorite is through a dynamic process [44]; redox reaction between the hypochlorite ions and the CDs. FT-IR spectrum shows that the signals of hydroxyl groups on the CD surface decreased significantly (Fig. 6B), supporting our suggestion that redox reactions occur between the surface groups of CDs and hypochlorite [48]. Aggregation of CDs induced

by hypochlorite is shown in the TEM image (Fig. 6C and D), which suggests that aggregation induced fluorescence mechanism cannot be ruled out. The fluorescence lifetimes of CD separately in the presence of hypochlorite and CBZ/hypochlorite are close, supporting our suggestion that the redox reaction of hypochlorite with CBZ before the oxidation of the surface groups in the CDs by hypochlorite.

4. Conclusion

The green emission CDs were synthesized through a one-step electrochemical synthesis. Further characterizations, such as absorbance spectroscopy, TEM, XPS, and FT-IR, demonstrated the formation of CDs. The CDs exhibited an emission peak at 520 nm under the excitations ($\lambda_{\text{ex}} = 420 \text{ nm}$). The hypochlorite was detected using the as-prepared CDs, with advantages of simplicity, sensitivity, and selectivity. Through the redox reaction of hypochlorite with CBZ, fluorescence quenching of CDs induced by hypochlorite is suppressed, allowing selective quantitation of CBZ down to 0.005 μM . The simple, selective and sensitive probes allow quantitation of hypochlorite and CBZ in real samples, with recoveries ranged from 96.3% to 108.9% and 103.1% to 107.7%, respectively. Our results show that the CD probes hold great potential for safety control of water and foods.

Conflict of interest

We declare that we do not have any commercial or associative interest that represents a conflict of interest in connection with this work.

Acknowledgments

This work was supported by the NTU and National Science and Technology Council of Taiwan, Taiwan (MOST 110-2113-M-143-001).

References

- [1] Cheng CW, Lo KM, Li MF, Chiu TC, Hu CC. Facile synthesis of dual-emission fluorescent carbon nanodots for a multi-functional probe. *RSC Adv* 2021;11:39958–65.
- [2] Han A, Hao S, Yang Y, Li X, Luo X, Fang G, et al. Perspective on recent developments of nanomaterial based fluorescent sensors: applications in safety and quality control of food and beverages. *J Food Drug Anal* 2020;28:486–507.
- [3] Zeng H, Li L, Ding Y, Zhuang Q. Simple and selective determination of 6-thioguanine by using polyethylenimine (PEI) functionalized carbon dots. *Talanta* 2018;178:879–85.
- [4] Wang CI, Wu WC, Periasamy AP, Chang HT. Electrochemical synthesis of photoluminescent carbon nanodots from glycine for highly sensitive detection of hemoglobin. *Green Chem* 2014;16:2509–14.

- [5] Mohapatra S, Bera M, Das R. Rapid “turn-on” detection of atrazine using highly luminescent N-doped carbon quantum dot. *Sensor Actuator B Chem* 2018;263:459–68.
- [6] An Q, Lin Q, Huang X, Zhou R, Guo X, Xu W, et al. Electrochemical synthesis of carbon dots with a Stokes shift of 309 nm for sensing of Fe³⁺ and ascorbic acid. *Dyes Pigments* 2021;185:108878.
- [7] Wei SC, Lin YW, Chang HT. Carbon dots as artificial peroxidases for analytical applications. *J Food Drug Anal* 2020;28:558–74.
- [8] Chu HW, Unnikrishnan B, Anand A, Lin YW, Huang CC. Carbon quantum dots for the detection of antibiotics and pesticides. *J Food Drug Anal* 2020;28:539–57.
- [9] Lee YS, Hu CC, Chiu TC. Electrochemical synthesis of fluorescent carbon dots for the selective detection of chlorotetracycline. *J Environ Chem Eng* 2022;10:107413.
- [10] Liu Y, Duan W, Song W, Liu J, Ren C, Wu J, et al. Red emission B, N, S-co-Doped carbon dots for colorimetric and fluorescent dual mode detection of Fe³⁺ ions in complex biological fluids and living cells. *ACS Appl Mater Interfaces* 2017;9:12663–72.
- [11] Roy P, Chen PC, Periasamy AP, Chen YN, Chang HT. Photoluminescent carbon nanodots: synthesis, physicochemical properties and analytical applications. *Mater Today* 2015;18:447–58.
- [12] Ross S, Wu RS, Wei SC, Ross GM, Chang HT. The analytical and biomedical applications of carbon dots and their future theranostic potential: a review. *J Food Drug Anal* 2020;28:677–95.
- [13] Lazarova V, Savoye P, Janex ML, Blatchley ER, Pommepuy M. Advanced wastewater disinfection technologies: state of the art and perspectives. *Water Sci Technol* 1999;40:203–13.
- [14] Marsche G, Hammer A, Oskolkova O, Kozarsky KF, Sattler W, Malle E. Hypochlorite-modified high density lipoprotein, a high affinity ligand to scavenger receptor class B, type I, impairs high density lipoprotein-dependent selective lipid uptake and reverse cholesterol transport. *J Biol Chem* 2002;277:32172–9.
- [15] Hu ZQ, Zhu JH, Gu Y, Hu WZ, Li M, Jiang Y. A sensitive and selective turn-on fluorescent probe for hypochlorous acid based on a thiorhodamine 6G amide, and its application in cellular imaging. *Microchim Acta* 2014;181:1401–6.
- [16] Habets JMW, Geursen-Reitsma AM, Stolz E, van Joost T. Sensitization to sodium hypochlorite causing hand dermatitis. *Contact Dermatitis* 1986;15:140–2.
- [17] Kishimoto N, Nishimura H. Effect of pH and molar ratio of pollutant to oxidant on a photochemical advanced oxidation process using hypochlorite. *Environ Technol* 2015;36:2436–42.
- [18] Banfi S, Montanari F, Quici S. Investigation on factors ruling catalytic efficiency and chemical stability of manganese(III) porphyrins in hypochlorous acid-olefin epoxidation: conditions for practical application. *J Org Chem* 1989;54:1850–9.
- [19] Magalhães LM, Segundo MA, Reis S, Lima JLFC, Estela JM, Cerdà V. Automatic in vitro determination of hypochlorous acid scavenging capacity exploiting multisyringe flow injection analysis and chemiluminescence. *Anal Chem* 2007;79:3933–9.
- [20] Zhang P, Zhang Q, Li S, Chen W, Guo X, Ding C. Enhanced fluorescence sensing of hypochlorous acid using serum albumin as a signal amplifier. *J Mater Chem B* 2019;7:1238–45.
- [21] Lopez LF, Lopez AG, Riba MV. HPLC method for simultaneous determination of fungicides: carbendazim, metalaxyl, folpet, and propiconazole in must and wine. *J Agric Food Chem* 1989;37:684–7.
- [22] Hernandez P, Ballesteros Y, Galan F, Hernandez L. Determination of carbendazim with a graphite electrode modified with silicone OV-17. *Electroanalysis* 1996;8:941–6.
- [23] Wu Q, Li Y, Wang C, Liu Z, Zang X, Zhou X, et al. Dispersive liquid–liquid microextraction combined with high performance liquid chromatography–fluorescence detection for the determination of carbendazim and thiabendazole in environmental samples. *Anal Chim Acta* 2009;638:139–45.
- [24] Yang Y, Wang H, Huang L, Zhang S, He Y, Gao Q, et al. Effects of superabsorbent polymers on the fate of fungicidal carbendazim in soils. *J Hazard Mater* 2017;328:70–9.
- [25] Sitarek K. Embryo-lethal and teratogenic effects of carbendazim in rats. *Teratog Carcinog Mutagen* 2001;21:335–40.
- [26] Jin Y, Zeng Z, Wu Y, Zhang S, Fu Z. Oral exposure of mice to carbendazim induces hepatic lipid metabolism disorder and gut microbiota dysbiosis. *Toxicol Sci* 2015;147:116–26.
- [27] Singh SB, Foster GD, Khan SU. Determination of thiophanate methyl and carbendazim residues in vegetable samples using microwave-assisted extraction. *J Chromatogr A* 2007;1148:152–7.
- [28] Guo Y, Guo S, Li J, Wang E, Dong S. Cyclodextrin–graphene hybrid nanosheets as enhanced sensing platform for ultra-sensitive determination of carbendazim. *Talanta* 2011;84:60–4.
- [29] Li Q, Li W. Determination of methyl thiophanate and carbendazim in fruits with ultraviolet spectrometer. *Deciduous Fruits* 2007;3:47–8.
- [30] Lezcano M, Al-Soufi W, Novo M, Rodríguez-Núñez E, Tato JV. Complexation of several benzimidazole-type fungicides with α - and β -cyclodextrins. *J Agric Food Chem* 2002;50:108–12.
- [31] Manisankar P, Selvanathan G, Vedhi C. Utilization of sodium montmorillonite clay-modified electrode for the determination of isoproturon and carbendazim in soil and water samples. *Appl Clay Sci* 2005;29:249–57.
- [32] Anastassiades M, Lehotay SJ, Štajnbaher D, Schenck FJ. Fast and easy multiresidue method employing acetonitrile extraction/partitioning and “dispersive solid-phase extraction” for the determination of pesticide residues in produce. *J AOAC Int* 2019;86:412–31.
- [33] Lin YS, Lin Y, Periasamy AP, Cang J, Chang HT. Parameters affecting the synthesis of carbon dots for quantitation of copper ions. *Nanoscale Adv* 2019;1:2553–61.
- [34] Bozetine H, Wang Q, Barras A, Li M, Hadjersi T, Szunerits S, et al. Green chemistry approach for the synthesis of ZnO–carbon dots nanocomposites with good photocatalytic properties under visible light. *J Colloid Interface Sci* 2016;465:286–94.
- [35] Abe Y, Hiasa K, Takeuchi M, Yoshida Y, Suzuki K, Akagawa Y. New surface modification of titanium implant with phospho-amino acid. *Dent Mater J* 2005;24:536–40.
- [36] Li OL, Chiba S, Wada Y, Panomsuwan G, Ishizaki T. Synthesis of graphitic-N and amino-N in nitrogen-doped carbon via a solution plasma process and exploration of their synergic effect for advanced oxygen reduction reaction. *J Mater Chem* 2017;5:2073–82.
- [37] Pillar-Little T, Kim DY. Differentiating the impact of nitrogen chemical states on optical properties of nitrogen-doped graphene quantum dots. *RSC Adv* 2017;7:48263–7.
- [38] Li J, Zuo G, Qi X, Wei W, Pan X, Su T, et al. Selective determination of Ag⁺ using Salecan derived nitrogen doped carbon dots as a fluorescent probe. *Mater Sci Eng C* 2017;77:508–12.
- [39] Tang X, Cao M, Bi C, Yan L, Zhang B. Research on a new surface activation process for electroless plating on ABS plastic. *Mater Lett* 2008;62:1089–91.
- [40] Liang YC, Zhao Q, Wu XY, Li Z, Lu YJ, Liu Q, et al. A ratiometric fluorescent nanoprobe based on quenched carbon dots–rhodamine B for selective detection of l-cysteine. *J Alloys Compd* 2019;788:615–22.
- [41] Ma L, Sun S, Wang Y, Jiang K, Zhu J, Li J, et al. A graphene quantum dot-based fluorescent nanoprobe for hypochlorite detection in water and in living cells. *Microchim Acta* 2017;184:3833–40.
- [42] Jiao Y, Meng Y, Lu W, Gao Y, Liu Y, Gong X, et al. Design of long-wavelength emission carbon dots for hypochlorous detection and cellular imaging. *Talanta* 2020;219:121170.
- [43] Lin YS, Chuang LW, Lin YF, Hu SR, Huang CC, Huang YF, et al. Development of fluorescent carbon nanoparticle-based probes for intracellular pH and hypochlorite sensing. *Chemodosensors* 2022;10:64.

- [44] Zhang Z, Pei K, Yang Q, Dong J, Yan Z, Chen J. A nanosensor made of sulfur–nitrogen co-doped carbon dots for “off–on” sensing of hypochlorous acid and Zn(II) and its bioimaging properties. *New J Chem* 2018;42:15895–904.
- [45] Li J, Yang X, Zhang D, Liu Y, Tang J, Li Y, et al. A fluorescein-based “turn-on” fluorescence probe for hypochlorous acid detection and its application in cell imaging. *Sensor Actuator B Chem* 2018;265:84–90.
- [46] Zhang R, Liang L, Meng Q, Zhao J, Ta HT, Li L, et al. Responsive upconversion nanoprobe for background-free hypochlorous acid detection and bioimaging. *Small* 2019;15:1803712.
- [47] Zhang C, Liu M, Li T, Liu S, Chen Q, Zhang J, et al. One-pot hydrothermal synthesis of dual-emission fluorescent carbon dots for hypochlorous acid detection. *Dyes Pigments* 2020;180:108507.
- [48] Li Y-X, Lee JY, Lee H, Hu CC, Chiu TC. Highly fluorescent nitrogen-doped carbon dots for selective and sensitive detection of Hg^{2+} and ClO^- ions and fluorescent ink. *J Photochem Photobiol, A* 2021;405:112931.